Journal of Solid State Chemistry **153,** 55–65 (2000)
doi:10.1006/jssc.2000.8739, available online at http://www.idealibrary.com on IDEAL®

Two New Thiophosphates with Interlocked Structures: $AgTi_2(PS_4)_3$ and $Ag_2NbTi_3P_6S_{25}$

J. Angenault, X. Cieren, G. Wallez, and M. Quarton[1]

Laboratoire de Cristallochimie du Solide, Université Pierre et Marie Curie — Paris VI, 4 place Jussieu, 75252 Paris cedex 05, France

Received January 18, 2000; in revised form March 27, 2000; accepted April 7, 2000; published online June 27, 2000

The crystal structures of $AgTi_2(PS_4)_3$ and $Ag_2NbTi_3P_6S_{25}$ were determined from single-crystal X-ray diffraction data. $AgTi_2(PS_4)_3$ crystallizes in the orthorhombic system, space group *Ccc*2 (no. 37), $a = 34.691(4)$ Å, $b = 20.018(2)$ Å, and $c = 11.576(2)$ Å, $V = 8039(4)$ Å^3, $Z = 16$. The structural skeleton is built up from TiS_6 octahedra and PS_4 tetrahedra linked to each other by edges. It exhibits very wide tunnels along the *c* axis. $Ag_2NbTi_3P_6S_{25}$ crystallizes in the orthorhombic system, space group *Pccn* (no. 56), $a = 22.609(2)$ Å, $b = 27.694(2)$ Å, and $c = 11.589(1)$ Å, $V = 7256(4)$ Å^3, $Z = 8$. The structure is made of edge-sharing TiS_6 octahedra, PS_4 tetrahedra, P_2S_6 bitetrahedra, and Nb_2S_{8+4} tetracapped trigonal biprisms. The Nb_2S_8 entity includes two disulfide anions $(S_2)^{2-}$ and an Nb^{IV}–Nb^{IV} bond. The formula of the compound can be written as $Ag_4^{I}Nb_2^{IV}Ti_6^{IV}(P_2S_6)^{2-}(PS_4)_{10}^{3-}(S_2)_2^{2-}$. Each of the two structures presents two interlocked sublattices of polyhedra chains linked together by bridging S–Ag–S bonds. For $AgTi_2(PS_4)_3$ the ionic conductivity measured along [001] is in agreement with a strong delocalization of Ag^+ ions in the wide tunnels. © 2000 Academic Press

Key Words: **thiophosphates; sulfurs; open structures; interlocked structures; ionic conductivity.**

INTRODUCTION

2D (layers) and 3D (tunnels) open-structure compounds exhibit generally good ionic conductivity, especially when mobile cations are monovalent (Li^+, Na^+, Ag^+) (1,2). So the transition metal sulfides MS_2 and thiophosphates MPS_3, with the same 2D structure type, are known as excellent intercalation materials (3,4). Other thiophosphates exhibit the MPS_3 structure type, like $A^IMP_2S_6$ with A = Cu (5,6) or Ag (7–10). The thiophosphates which host large alkali cations lead to original low-dimensional structures due to the separation of anionic polyhedra layers: $RbVP_2S_7$ (11) and $KNiPS_4$ (12). In contrast, a 3D structure with wide tunnels is obtained with Na^+ for $NaTi_2(PS_4)_3$ (13).

In this paper we present the homologous silver compounds $AgTi_2(PS_4)_3$ and $Ag_2NbTi_3P_6S_{25}$ with original structures that shows many similar features. In addition to crystal structure determinations, we report ionic conductivity measurements for $NaTi_2(PS_4)_3$ and $AgTi_2(PS_4)_3$ compounds.

SYNTHESIS

The compounds were prepared by direct synthesis from Ag_2S, Nb, Ti, P, and S. Ag_2S was obtained by precipitation of silver acetate (CH_3COOAg, Fluka, 99.0%) in thioacetamide solution. Powders of the elements were commercially obtained from Aldrich: Nb metal (99.9%), Ti metal (99.9%), red P (99.99%), and S (99.98%).

$AgTi_2(PS_4)_3$

Stoichiometric amounts of starting materials were mixed and then put in a dry evacuated sealed silica tube. After a slow heating to 600°C (2°C.hr^{-1}), 3 days at 600°C, and a slow cooling (5°C.hr^{-1}), we obtained small dark entangled needles with metallic luster. These air-sensitive single crystals were kept and handled in a dry glovebox, stored in a sealed-off Lindemann glass capillary.

$Ag_2NbTi_3P_6S_{25}$

Crystals were synthesized by mixing powders of Ag_2S, Nb, Ti, red P, and S in stoichiometric amounts in order to obtain the hypothetical "$AgNbTi(PS_4)_3$" compound. The same thermal treatment as above was used. Finally, in addition to different known niobium thiophosphates like $Nb_4P_2S_{21}$ (14) and Nb_2PS_{10} (15), we isolated black single crystals of $Ag_2NbTi_3P_6S_{25}$.

STRUCTURE REFINEMENTS

The analytical and crystallographic data are gathered in Table 1. The recorded intensities were first corrected for the

[1] To whom correspondence should be addressed. Fax: 33-1 44 27 25 48. E-mail: mq@ccr.jussieu.fr.

0022-4596/00 $35.00

TABLE 1
Data Collection and Refinement Conditions for $AgTi_2(PS_4)_3$ and $Ag_2NbTi_3P_6S_{25}$

	$AgTi_2(PS_4)_3$	$Ag_2NbTi_3P_6S_{25}$
	Crystal Data	
Crystal system	Orthorhombic	Orthorhombic
Space group	*Ccc*2 (no. 37)	*Pccn* (no. 56)
Unit cell dimensions	$a = 34.691(4)$ Å	$a = 22.609(2)$ Å
	$b = 20.018(2)$ Å	$b = 27.694(2)$ Å
	$c = 11.576(2)$ Å	$c = 11.589(1)$ Å
	$V = 8039(4)$ Å^3	$V = 7256(4)$ Å^3
Theoretical density	2.252 g.cm^{-3} ($Z = 16$)	2.636 g.cm^{-3} ($Z = 8$)
	Data Collection	
Temperature	293 K	
Diffractometer	Enraf-Nonius CAD4	
Radiation (graphite monochromator)	Mo$K\alpha - \lambda = 0.71069$ Å	
Scans/speed	ω–2θ/1.7 to 20.1°.min^{-1}	
2θ range/scan breadth	2–44°/8 + 0.345 tan θ	
No. of standard reflections/frequency	3/60 min	
Crystal size	$0.5 \times 0.3 \times 0.2$ mm^3	$0.4 \times 0.2 \times 0.2$ mm^3
Linear absorption coefficient	$\mu = 3.14$ mm^{-1}	$\mu = 3.62$ mm^{-1}
$h/k/l$ ranges	0–40/0–23/0–13	0–22/0–27/0–11
No. of observed reflections	3741	6285
	Structure Refinement	
Transmission factors (16)	$0.399 \le \tau = 0.552$	$0.495 \le \tau \le 0.617$
No. of parameters	370	349
Reliability factors	$R = 0.079$	$R = 0.085$
$w = 1/\sigma^2$	$R_w = 0.054$	$R_w = 0.061$
Extinction parameter	$g = 0.362(9) \times 10^{-6}$	$g = 0.25(1) \times 10^{-6}$
Electronic residues (min./max.)	−0.39/0.54 e.Å^{-3}	−0.82/0.69 e.Å^{-3}

Lorentz and polarization factors, then for the absorption phenomena (16). A centrosymmetry test (17) was achieved from the diffracted intensities of $AgTi_2(PS_4)_3$ and it showed that the noncentrosymmetric space group *Ccc*2 was retained. The atomic positions were determined by direct methods with the SHELXS-86 program (18) and refined with the ORXFLS program (19), taking into account the secondary extinction (20). Sites of Ag atoms are not completely occupied in both structures and consequently in the final refinement the sum of the occupancies of these sites was constrained to the values needed to charge balance the formulae. Fairly high values of reliability factors (Table 1) are due to the bad crystal quality of our samples, which generated very weak diffracted intensities at high angles and non-negligible background.

Atomic coordinates and thermal parameters for $AgTi_2(PS_4)_3$ and $Ag_2NbTi_3P_6S_{25}$ are gathered in Tables 2 and 4 respectively. Main interatomic distances and interbond angles for these two compounds are gathered in Tables 3 and 5 respectively.

STRUCTURES DESCRIPTION

The two structures are built up from irregular TiS_6 octahedra and PS_4 tetrahedra, sharing only edges alternatively to form polyhedra chains. Table 6 gathers geometric data for these polyhedra for the two compounds. The mean Ti–S and P–S distances indicate that the cations are in the

TABLE 2
Occupation Factors, Fractional Atomic Coordinates, and Equivalent Isotropic Displacement Parameters for $AgTi_2(PS_4)_3$

Atoms	τ	x	y	z	U_{eq}(Å^2)[a]
Ti(1)	1	0.34042(9)	0.4995(2)	0	0.030(2)
Ti(2)	1	0.3448(1)	0.1936(2)	0.4962(2)	0.035(2)
Ti(3)	1	0.3193(1)	0.1274(1)	0.9918(2)	0.028(2)
Ti(4)	1	0.4790(1)	0.3089(2)	0.9864(2)	0.043(2)
P(1)	1	0.3384(1)	0.3486(2)	0.4980(3)	0.033(3)
P(2)	1	0.2629(1)	0.4251(2)	0.9996(3)	0.029(3)
P(3)	1	0.4146(2)	0.4156(2)	0.9930(3)	0.033(3)
P(4)	1	0.3487(1)	0.1536(2)	0.7537(4)	0.034(3)
P(5)	1	0.3442(1)	0.1396(2)	0.2514(4)	0.034(3)
P(6)	1	0.4961(1)	0.2766(2)	0.2393(3)	0.034(3)
S(11)	1	0.3596(1)	0.5927(2)	0.1232(3)	0.038(3)
S(12)	1	0.2993(1)	0.2795(2)	0.5557(4)	0.045(4)
S(13)	1	0.3793(1)	0.2922(2)	0.4231(4)	0.035(3)
S(14)	1	0.3157(1)	0.5866(2)	0.8788(3)	0.040(3)
S(21)	1	0.2836(1)	0.4825(2)	0.1277(4)	0.041(3)
S(22)	1	0.2538(1)	0.1641(2)	0.0580(4)	0.044(3)
S(23)	1	0.2821(1)	0.0345(2)	0.9181(4)	0.043(3)
S(24)	1	0.3086(1)	0.4177(2)	0.8855(4)	0.052(4)
S(31)	1	0.4141(1)	0.3260(2)	0.9147(3)	0.039(3)
S(32)	1	0.3980(1)	0.4911(2)	0.8831(3)	0.045(3)
S(33)	1	0.4682(1)	0.4246(2)	0.0494(4)	0.045(4)
S(34)	1	0.3779(1)	0.4217(2)	0.1281(3)	0.042(3)
S(41)	1	0.3124(1)	0.1171(2)	0.6211(3)	0.055(4)
S(42)	1	0.3695(1)	0.0832(2)	0.8643(3)	0.041(3)
S(43)	1	0.3889(1)	0.1983(2)	0.6581(4)	0.052(4)
S(44)	1	0.3165(1)	0.2171(2)	0.8522(3)	0.045(3)
S(51)	1	0.3367(1)	0.0539(2)	0.1538(4)	0.051(4)
S(52)	1	0.3494(1)	0.2070(2)	0.1192(3)	0.041(3)
S(53)	1	0.3882(1)	0.1335(2)	0.3664(3)	0.046(3)
S(54)	1	0.2980(1)	0.1646(2)	0.3524(4)	0.058(4)
S(61)	1	0.4800(1)	0.2110(2)	0.8539(3)	0.034(3)
S(62)	1	0.5191(1)	0.3567(2)	0.8334(3)	0.048(4)
S(63)	1	0.4515(1)	0.2433(2)	0.1450(4)	0.048(4)
S(64)	1	0.5345(1)	0.3060(2)	0.1108(4)	0.044(3)
Ag(1)	0.570(6)	0.38430(7)	0.30921(9)	0.2127(2)	0.046(2)
Ag(2)	0.301(6)	0.2249(1)	0.5202(2)	0.2161(4)	0.059(4)
Ag(3)	0.206(6)	0.4025(2)	0.3259(3)	0.7115(5)	0.048(5)
Ag(4)	0.34(1)	0.5060(6)	0.0792(4)	0.131(3)	0.64(4)
Ag(5)	0.23(1)	0.4484(6)	0.987(1)	0.075(4)	0.61(6)
Ag(6)	0.203(9)	0.492(1)	0.984(1)	0.930(4)	0.61(6)
Ag(7)	0.15(1)	0.4555(7)	0.051(1)	0.175(8)	0.7(1)

[a] $U_{eq} = (\sum_i U_{ii})/3$.

TABLE 3
Bond Distances (Å) and Interbond Angles (°) in the $AgTi_2(PS_4)_3$ Structure

Ti(1)	S(24)	S(14)	S(32)	S(11)	S(21)	S(34)
S(24)	**2.378(6)**	3.3925(8)	3.4318(7)	4.7925(9)	3.2098(9)	3.6964(8)
S(14)	90.5(2)	**2.397(5)**	3.4370(7)	3.2147(9)	3.7268(8)	4.8862(8)
S(32)	91.4(2)	91.1(2)	**2.419(5)**	3.6927(8)	4.879(1)	3.2331(9)
S(11)	168.1(2)	83.3(2)	98.9(2)	**2.441(5)**	3.43712(6)	3.4806(8)
S(21)	82.5(2)	99.4(2)	167.9(2)	88.4(2)	**2.488(5)**	3.4907(8)
S(34)	98.2(2)	168.9 (2)	81.9(2)	89.3(2)	88.6(2)	**2.512(5)**

Ti(2)	S(41)	S(54)	S(43)	S(12)	S(53)	S(13)
S(41)	**2.388(5)**	3.291(1)	3.1411(6)	3.3698(8)	3.9644(9)	4.7876(8)
S(54)	86.9(2)	**2.398(5)**	4.787(2)	3.2917(7)	3.1948(8)	3.8913(7)
S(43)	81.6(2)	167.2(2)	**2.420(5)**	3.7014(7)	3.618(2)	3.3226(8)
S(12)	88.6(2)	85.9(2)	99.4(2)	**2.435(5)**	4.7814(8)	3.1807(7)
S(53)	110.3(2)	82.6(2)	96.1(2)	157.1(2)	**2.444(5)**	3.2587(8)
S(13)	162.3(2)	106.6(2)	85.9(2)	81.1(2)	83.4(2)	**2.457(5)**

Ti(3)	S(52)	S(44)	S(23)	S(42)	S(51)	S(22)
S(52)	**2.409(5)**	3.300(1)	4.7742(8)	3.9153(9)	3.1223(8)	3.4956(8)
S(44)	86.3(2)	**2.418(5)**	3.9208(6)	3.2526(6)	4.832(1)	3.3947(7)
S(23)	162.9(2)	108.3(2)	**2.419(5)**	3.2449(7)	3.3436(8)	3.2098(9)
S(42)	107.4(2)	83.9(2)	83.6(2)	**2.448(5)**	3.587(2)	4.8729(9)
S(51)	79.8(2)	164.5(2)	86.6(2)	93.9(2)	**2.459(5)**	3.7897(7)
S(22)	90.6(2)	87.2(2)	81.4(2)	159.2(2)	99.5(2)	**2.506(5)**

Ti(4)	S(64)	S(31)	S(62)	S(63)	S(33)	S(61)
S(64)	**2.404(5)**	4.770(1)	3.410(1)	3.1659(7)	3.3797(6)	4.0051(8)
S(31)	162.2(2)	**2.424(5)**	3.8123(9)	3.3964(8)	3.1375(5)	3.3212(6)
S(62)	89.3(2)	103.0(2)	**2.448(5)**	3.3497(7)	3.3497(7)	3.2257(7)
S(63)	81.4(2)	88.3(2)	166.7(2)	**2.450(5)**	3.8382(9)	3.571(2)
S(33)	88.1(2)	80.0(2)	86.2(2)	102.9(2)	**2.457(6)**	4.856(1)
S(61)	109.8(2)	85.0(2)	81.6(2)	92.6(2)	158.0(2)	**2.490(5)**

P(1)	S(11)	S(13)	S(12)	S(14)
S(11)	**2.006(6)**	3.3385(7)	3.3955(6)	3.2147(9)
S(13)	112.6(2)	**2.008(6)**	3.1807(7)	3.3181(6)
S(12)	113.7(3)	103.2(3)	**2.049(6)**	3.4200(7)
S(14)	104.8(3)	109.6(3)	113.0(3)	**2.051(6)**

P(2)	S(23)	S(22)	S(21)	S(24)
S(23)	**1.995(6)**	3.2129(6)	3.3459(7)	3.3115(8)
S(22)	107.3(3)	**1.996(6)**	3.3104(7)	3.3710(6)
S(21)	113.3(3)	111.5(3)	**2.010(6)**	3.2098(9)
S(24)	109.1(5)	112.0(3)	103.7(3)	**2.070(7)**

P(3)	S(33)	S(31)	S(34)	S(32)
S(33)	**1.980(7)**	3.1375(5)	3.2631(8)	3.3773(6)
S(31)	103.7(3)	**2.009(6)**	3.3690(7)	3.3706(8)
S(34)	109.3(3)	113.5(3)	**2.020(6)**	3.2331(9)
S(32)	113.6(3)	112.0(3)	104.9(3)	**2.057(6)**

P(4)	S(43)	S(42)	S(44)	S(41)
S(43)	**1.992(6)**	3.3853(7)	3.3898(7)	3.1411(6)
S(42)	114.4(3)	**2.035(6)**	3.2526(6)	3.5081(8)
S(44)	114.4(3)	105.9(3)	**2.041(6)**	3.3447(8)
S(41)	99.7(3)	115.4(3)	107.1(3)	**2.116(6)**

P(5)	S(53)	S(54)	S(52)	S(51)
S(53)	**2.030(6)**	3.1948(8)	3.4896(8)	3.4337(7)
S(54)	103.2(3)	**2.046(6)**	3.3448(8)	3.4639(6)
S(52)	117.6(3)	109.6(3)	**2.049(5)**	3.1223(8)
S(51)	113.7(3)	114.6(3)	98.6(3)	**2.070(6)**

P(6)	S(62)	S(63)	S(61)	S(64)
S(62)	**2.009(6)**	3.3092(6)	3.2257(7)	3.3353(7)
S(63)	110.9(3)	**2.009(6)**	3.4510(7)	3.1659(7)
S(61)	105.6(2)	116.8(3)	**2.042(5)**	3.4342(8)
S(64)	109.3(3)	101.4(3)	112.8(3)	**2.081(6)**

TABLE 3—*Continued*

Ag(1)	S(13)	S(34)	S(52)	S(63)
S(13)	**2.466(5)**	4.289(1)	4.045(2)	4.1962(9)
S(34)	120.8(2)	**2.467(4)**	4.412(1)	4.3962(8)
S(52)	105.6(2)	120.6(2)	**2.613(4)**	3.6298(9)
S(63)	105.7(2)	113.3(2)	84.3(2)	**2.792(5)**

Ag(2)	S(23)	S(21)	S(41)	S(51)
S(23)	**2.368(6)**	4.192(1)	3.957(1)	4.0101(9)
S(21)	123.0(3)	**2.401(6)**	4.2832(8)	4.247(2)
S(41)	106.2(2)	118.7(3)	**2.578(6)**	3.5450(8)
S(51)	104.5(3)	112.7(2)	84.4(2)	**2.698(7)**

Ag(3)	S(31)	S(11)	S(64)	S(43)
S(31)	**2.387(7)**	4.197(1)	3.964(2)	4.0152(9)
S(11)	121.1(3)	**2.433(7)**	4.1996(9)	4.324(1)
S(64)	108.1(3)	116.4(3)	**2.508(8)**	3.4672(6)
S(43)	105.0(3)	115.8(3)	84.0(3)	**2.670(8)**

Ag(4)–S(61)	3.72(3)
S(63)	3.79(2)
S(61)	4.25(3)
S(43)	4.37(2)
S(64)	4.65(2)
S(53)	4.90(4)

Ag(5)–S(53)	4.00(4)
S(42)	4.14(3)
S(51)	4.20(4)
S(43)	4.36(2)
S(42)	4.55(5)
S(53)	4.93(5)

Ag(6)–S(61)	4.10(3)
S(53)	4.37(3)
S(61)	4.66(3)
S(42)	4.77(5)

Ag(7)–S(53)	3.62(6)
S(63)	3.87(3)
S(51)	4.13(3)
S(61)	4.43(7)
S(42)	4.57(5)
S(42)	4.72(8)
S(52)	4.88(2)
S(61)	4.98(7)

Ti^{IV} and P^{V} states, according to their ionic radii (21). Some of the Ag atoms in both of the structures exhibit high displacement parameters in agreement with (i) the d^{10} electronic configuration of the Ag^+ cations (22) and (ii) their weak localization in the tunnels of the structural frameworks.

$AgTi_2(PS_4)_3$ Structure

Each TiS_6 octahedron shares three nonadjacent edges with three PS_4 tetrahedra to build up three polyhedra chains expanding along a pseudo-three-fold axis, with continuations around TiS_6 octahedron (Fig. 1a). The so-formed 3D interconnected chains sublattice is $c/2$ duplicated with the glide plane perpendicular to b. These two independent and interlocked sublattices make up a 3D skeleton and arrange cavities and wide tunnels in which Ag^+ cations are located.

Ag(1) to Ag(3) atoms partially occupy distorted tetrahedral sites with Ag–S distances ranging from 2.368 to 2.792 Å (Table 3) in agreement with the corresponding values in the $Ag_4P_2S_7$ (23) and $Ag_2P_2S_6$ (24) thiophosphates. Ag(4) to Ag(7) atoms are located in the wide tunnels parallel to the c axis and present different coordinations (Table 3). Taking into account the weakness of the Ag–S bonds (Ag–S $\geq$ 3.62Å) and their high thermal agitation (Table 2), more particularly along [001] (U_{33} is about 10 times larger than U_{11} and U_{22}), one can say that these Ag^+ cations are delocalized in the wide tunnels.

$Ag_2NbTi_3P_6S_{25}$ Structure

The structural skeleton presents common features with the $AgTi_2(PS_4)_3$ one. However, in one of the three chains developing from the Ti(1)S_6 octahedra, an Nb_2S_{8+4} entity takes the place of the Ti(4)S_6 octahedron (Fig. 2a). This centrosymmetric Nb_2S_{8+4} entity is built up from two trigonal NbS_6 prisms sharing a lateral face; the two other lateral faces are capped with a sulfur atom (Fig. 3). Nb–$S_{extraprism}$ distances (2.604 and 2.611Å) are similar to Nb–$S_{intraprism}$ distances (2.461 to 2.675Å) (Table 5). The Nb–Nb distance is equal to 2.861(2)Å. The two lengths of the S(1)–S(2) edges of the common face are very different: 1.957(6) and 3.559(5)Å. These two sulfur atoms S(1) and S(2) belong only to the Nb_2S_8 biprism.

The tetracapped trigonal biprisms Nb_2S_{12} share two opposite edges with P_2S_6 entities to build alternate chains parallel to a (Fig. 3). The centrosymmetric entity P_2S_6 results from sharing the S(41)–S(41) edge (3.110Å) of two P(4)S_4 tetrahedra (Fig. 3). The P(4)–P(4) distance is equal to 2.838(1)Å.

The structure can be described as a succession of (010) layers made up of alternate chains of TiS_6 octahedra and PS_4 tetrahedra. Cohesion between layers is assumed to occur by Nb_2S_{12} bipolyhedra, building up two independent and interlocked sublattices.

Ag(1) to Ag(3) atoms, with a coordination number of 3, are located in different cavities of the structural skeleton. As noticed in the other structure, some Ag^+ cations are strongly delocalized in the tunnels parallel to c; besides, these

TABLE 4
Occupation Factors, Fractional Atomic Coordinates, and Equivalent Isotropic Displacement Parameters for $Ag_2NbTi_3P_6S_{25}$

Atoms	τ	x	y	z	$U_{eq}(Å^2)^a$
Nb	1	0.00352(5)	0.97566(4)	0.89133(8)	0.0196(6)
Ti(1)	1	0.98936(9)	0.75007(9)	0.8579(2)	0.012(1)
Ti(2)	1	0.7194(1)	0.89428(8)	0.8537(2)	0.018(1)
Ti(3)	1	0.7820(1)	0.12696(9)	0.6273(2)	0.016(1)
P(1)	1	0.9953(2)	0.8585(1)	0.8469(2)	0.015(2)
P(2)	1	0.1084(1)	0.6946(1)	0.8731(3)	0.017(2)
P(3)	1	0.8809(1)	0.6845(1)	0.8528(2)	0.022(2)
P(4)	1	0.0074(2)	0.0011(1)	0.6216(2)	0.013(2)
P(5)	1	0.2421(1)	0.8928(1)	0.1106(2)	0.015(2)
P(6)	1	0.7446(2)	0.9168(1)	0.1069(3)	0.020(2)
S(11)	1	0.9404(2)	0.9089(1)	0.7839(3)	0.021(2)
S(12)	1	0.0661(1)	0.8968(1)	0.9106(2)	0.021(2)
S(13)	1	0.9567(2)	0.8165(1)	0.9734(2)	0.018(2)
S(14)	1	0.0236(2)	0.8108(1)	0.7307(3)	0.021(2)
S(21)	1	0.0759(1)	0.7449(1)	0.9768(2)	0.018(2)
S(22)	1	0.0449(1)	0.6905(1)	0.7449(2)	0.020(2)
S(23)	1	0.8092(2)	0.2095(1)	0.6903(3)	0.024(2)
S(24)	1	0.8806(2)	0.1282(1)	0.5467(3)	0.024(2)
S(31)	1	0.7045(1)	0.8096(1)	0.9148(2)	0.019(2)
S(32)	1	0.9390(1)	0.6924(1)	0.9827(2)	0.021(2)
S(33)	1	0.1182(1)	0.1184(1)	0.7166(3)	0.022(2)
S(34)	1	0.9024(1)	0.7366(1)	0.7390(2)	0.018(2)
S(41)	1	0.0228(1)	0.0529(1)	0.4922(2)	0.021(2)
S(42)	1	0.0782(1)	0.9794(1)	0.7124(2)	0.012(2)
S(43)	1	0.9471(1)	0.0246(1)	0.7343(2)	0.022(2)
S(51)	1	0.2210(2)	0.8335(1)	0.0110(3)	0.027(2)
S(52)	1	0.7010(1)	0.1278(2)	0.7607(2)	0.032(2)
S(53)	1	0.8277(2)	0.0821(1)	0.7911(3)	0.025(2)
S(54)	1	0.7724(2)	0.0603(1)	0.5031(3)	0.035(2)
S(61)	1	0.7194(2)	0.6391(1)	0.7056(3)	0.045(3)
S(62)	1	0.7774(2)	0.9629(1)	0.2260(3)	0.037(2)
S(63)	1	0.8014(1)	0.8950(1)	0.9849(3)	0.030(2)
S(64)	1	0.6758(2)	0.9398(1)	0.0143(3)	0.026(2)
S(1)	1	0.0907(2)	0.0026(1)	0.0034(3)	0.023(2)
S(2)	1	0.0458(2)	0.0558(1)	0.9350(2)	0.028(2)
Ag(1)	1 .00(4)	0.09146(8)	0.8638(1)	0.1002(1)	0.174(2)
Ag(2)	0.45(4)	0.8924(4)	0.8675(3)	0.6342(8)	0.43(1)
Ag(3)	0.52(4)	0.1009(3)	0.8791(3)	0.6668(4)	0.296(7)
Ag(4)	0.03(2)	1/4	1/4	0.71(2)	0.5(1)

[a] $U_{eq} = (\sum_i U_{ii})/3$.

tunnels are narrower than in $AgTi_2(PS_4)_3$ compound and therefore allow fewer Ag(4) atoms (Table 4).

IONIC CONDUCTIVITY

The presence of delocalizable Ag^+ ions in the wide tunnels led us to measure the ionic conductivity of $AgTi_2(PS_4)_3$ and to compare it with that of the isotypic compound $NaTi_2(PS_4)_3$.

Total conductivity was measured by the complex impedance method (25) using an HP 4284A impedancemeter, with frequencies ranging from 20 Hz to 1 MHz. Electronic conductivity was studied with blocking electrodes at low voltage (26). We measured the conductivity at different temperatures, ranging from 50 to 350°C, under argon atmosphere, on two types of samples:

— single crystals elongated along c ($\approx 0.5 \times 0.5 \times 4\ mm^3$), fixed on alumina substrate and fitted with platinum lacquer, between two platinum electrodes;

— packed powder chips (diameter ≈ 8 mm, thickness ≈ 2 mm), heated at 450°C during 12 hr under purified argon atmosphere. Powders were obtained by heating at 500°C stoichiometric amounts of $Ag_2S(Na_2S) + Ti + P + S$ in a dry evacuated sealed silica tube, then analyzed by X-ray diffraction.

The values of the total conductivity follow an Arrhenius law (Fig. 4). Activation energies were calculated from slopes of $\ln(\sigma T) = f(1/T)$. The maximum of the electronic conductivity part is never over 0.3%, so one can consider the electric conductivity as an almost fully ionic one.

The high values of conductivity along [001] for single crystals (Table 7) are certainly due to the high ionic mobility along the wide tunnels. The equivalent performances for $AgTi_2(PS_4)_3$ and $NaTi_2(PS_4)_3$ can be explained, on one hand, by the similar free monovalent ion concentrations (46% of Ag^+ in $AgTi_2(PS_4)_3$ and 43% of Na^+ in $NaTi_2(PS_4)_3$ are located in the tunnels), and on the other hand, by the very high "tunnels diameter/mobile ions radius" ratio. So the determining factors for the ionic conductivity (number and charge of ions, mobility) are similar for the two compounds.

The conductivity of chips is weak with a high activation energy (Table 7) because of the disorientation of microcrystals and the strong anisotropy of the ionic migration ways. At high temperature, $AgTi_2(PS_4)_3$ is a better conductor than the homologous compound $NaTi_2(PS_4)_3$.

DISCUSSION

The $AgTi_2(PS_4)_3$ and $NaTi_2(PS_4)_3$ structures are isotypic but the "$Ti_2(PS_4)_3$" skeleton is slightly distorted in the former: Ti(n)–Ti(1)–Ti(m) angles are equal to 116.05(1), 116.90(2), and 126.98(1)° instead of exactly 120° in the sodium compound (13). In the two structures, about 45% of monovalent atoms (Na or Ag) are located in wide tunnels, forming very weak bonds: Na–S $\geq$ 3.88Å (13) and Ag–S $\geq$ 3.62Å (Table 3). Thus we can assume that the distortion results from the other monovalent atoms located in tetrahedral sites, keeping in mind that Ag–S links are less ionic than Na–S ones. So Na^+ ions are found in narrow tunnels, surrounded by bulky and nearly regular sulfur tetrahedra, $\langle Na–S \rangle = 3.01Å > r_{Na^+} + r_{S^{2-}} \approx 2.80$ Å (13, 21), without noticeable constrictions of the framework. Ag–S

TABLE 5
Bond Distances (Å) and Interbond Angles (°) in the $Ag_2NbTi_3P_6S_{25}$ Structure

Ti(1)	S(14)	S(13)	S(21)	S(34)	S(32)	S(22)
S(14)	**2.368(5)**	3.198(4)	3.588(5)	3.428(5)	4.790(5)	3.371(5)
S(13)	84.4(2)	**2.392(4)**	3.345(5)	3.713(5)	3.461(5)	4.812(5)
S(21)	97.7(2)	88.6(2)	**2.397(4)**	4.799(5)	3.420(5)	3.159(4)
S(34)	91.2(2)	100.7(2)	167.7(2)	**2.430(4)**	3.187(4)	3.466(5)
S(32)	171.2(2)	91.6(2)	90.0(2)	81.80(1)	**2.437(4)**	3.652(5)
S(22)	88.7(2)	167.0(2)	81.3(2)	90.47(1)	96.67(1)	**2.452(5)**

Ti (2)	S(61)	S(63)	S(62)	S(33)	S(64)	S(31)
S(61)	**2.389(5)**	3.404(5)	3.123(6)	3.823(6)	4.815(5)	3.294(5)
S(63)	90.7(2)	**2.398(4)**	3.964(5)	4.769(5)	3.118(5)	3.324(5)
S(62)	81.2(2)	111.2(2)	**2.408(5)**	3.327(6)	3.562(5)	4.792(6)
S(33)	104.2(2)	158.8(2)	86.4(2)	**2.454(4)**	3.384(5)	3.177(5)
S(64)	167.3(2)	79.9(2)	94.2(2)	87.2(2)	**2.455(4)**	3.840(5)
S(31)	85.3(2)	86.1(2)	158.1(2)	80.3(2)	102.4(2)	**2.473(5)**

Ti(3)	S(54)	S(51)	S(52)	S(24)	S(23)	S(53)
S(54)	**2.352(5)**	3.167(6)	3.876(5)	3.129(5)	4.740(6)	3.616(5)
S(51)	84.0(2)	**2.381(4)**	3.356(5)	3.822(5)	3.293(5)	4.853(5)
S(52)	109.4(2)	89.2(2)	**2.397(4)**	4.760(5)	3.431(6)	3.153(5)
S(24)	82.0(2)	105.5(2)	162.5(2)	**2.418(5)**	3.230(5)	3.330(5)
S(23)	158.1(2)	85.3(2)	89.5(2)	82.6(2)	**2.476(5)**	3.740(5)
S(53)	96.5(2)	169.0(2)	80.3(2)	85.3(2)	97.6(2)	**2.494(4)**

Nb–S(2)	2.461(4)	Nb–S(2)	2.469(4)	Nb–S(1)	2.477(4)
S(1)	2.528(4)	S(43)	2.604(4)	S(12)	2.611(4)
S(11)	2.648(4)	S(42)	2.675(4)		

P(1)	S(14)	S(11)	S(12)	S(13)
S(14)	**1.992(5)**	3.359(5)	3.307(5)	3.198(4)
S(11)	114.4(2)	**2.004(5)**	3.216(5)	3.392(5)
S(12)	109.5(3)	104.7(2)	**2.057(5)**	3.405(5)
S(13)	104.0(2)	112.9(2)	114.4(2)	**2.065(5)**

P(2)	S(21)	S(23)	S(22)	S(24)
S(21)	**1.981(5)**	3.385(5)	3.159(4)	3.388(6)
S(23)	114.5(3)	**2.043(5)**	3.422(5)	3.230(5)
S(22)	102.5(2)	112.6(2)	**2.069(5)**	3.412(5)
S(24)	113.3(2)	103.3(2)	110.8(3)	**2.075(6)**

P(3)	S(33)	S(32)	S(34)	S(31)
S(33)	**2.001(5)**	3.347(5)	3.345(5)	3.177(5)
S(32)	113.2(3)	**2.009(5)**	3.187(4)	3.338(5)
S(34)	112.9(2)	104.8(2)	**2.013(5)**	3.410(5)
S(31)	102.7(2)	110.0(2)	113.4(3)	**2.066(5)**

P(4)	S(43)	S(42)	S(41)	S(41)
S(43)	**1.997(5)**	3.228(5)	3.379(5)	3.457(5)
S(42)	107.4(2)	**2.008(5)**	3.496(5)	3.411(5)
S(41)	111.0(2)	116.5(2)	**2.103(5)**	3.110(8)
S(41)	114.8(3)	112.0(2)	95.2(2)	**2.107(5)**

P(5)	S(54)	S(52)	S(51)	S(53)
S(54)	**1.973(5)**	3.428(5)	3.167(6)	3.394(5)
S(52)	116.8(3)	**2.051(5)**	3.356(5)	3.153(5)
S(51)	103.4(2)	109.3(3)	**2.063(5)**	3.455(5)
S(53)	114.2(3)	99.9(2)	113.6(2)	**2.067(5)**

P(6)	S(64)	S(63)	S(61)	S(62)
S(64)	**1.994(5)**	3.118(5)	3.266(6)	3.421(5)
S(63)	102.5(2)	**2.005(5)**	3.297(6)	3.412(5)
S(61)	109.4(3)	110.5(3)	**2.008(5)**	3.123(6)
S(62)	116.9(3)	115.9(3)	101.7(2)	**2.020(5)**

Ag(1)	S(12)	S(22)	S(53)
S(12)	**2.449(4)**	4.593(5)	4.250(5)
S(22)	137.1(2)	**2.486(4)**	4.182(6)
S(53)	111.9(2)	108.1(2)	**2.679(4)**

Ag(2)	S(11)	S(32)	S(61)
S(11)	**2.345(6)**	4.478(5)	3.956(6)
S(32)	128.0(4)	**2.634(7)**	4.657(5)
S(61)	104.0(4)	122.9(4)	**2.67(2)**

Ag(3)	S(52)	S(24)	S(14)
S(52)	**2.421(8)**	3.793(5)	4.356(6)
S(24)	100.4(3)	**2.518(6)**	4.227(5)
S(14)	117.3(3)	108.9(3)	**2.678(7)**

Ag(4)–S(31) 2.4(2) × 2

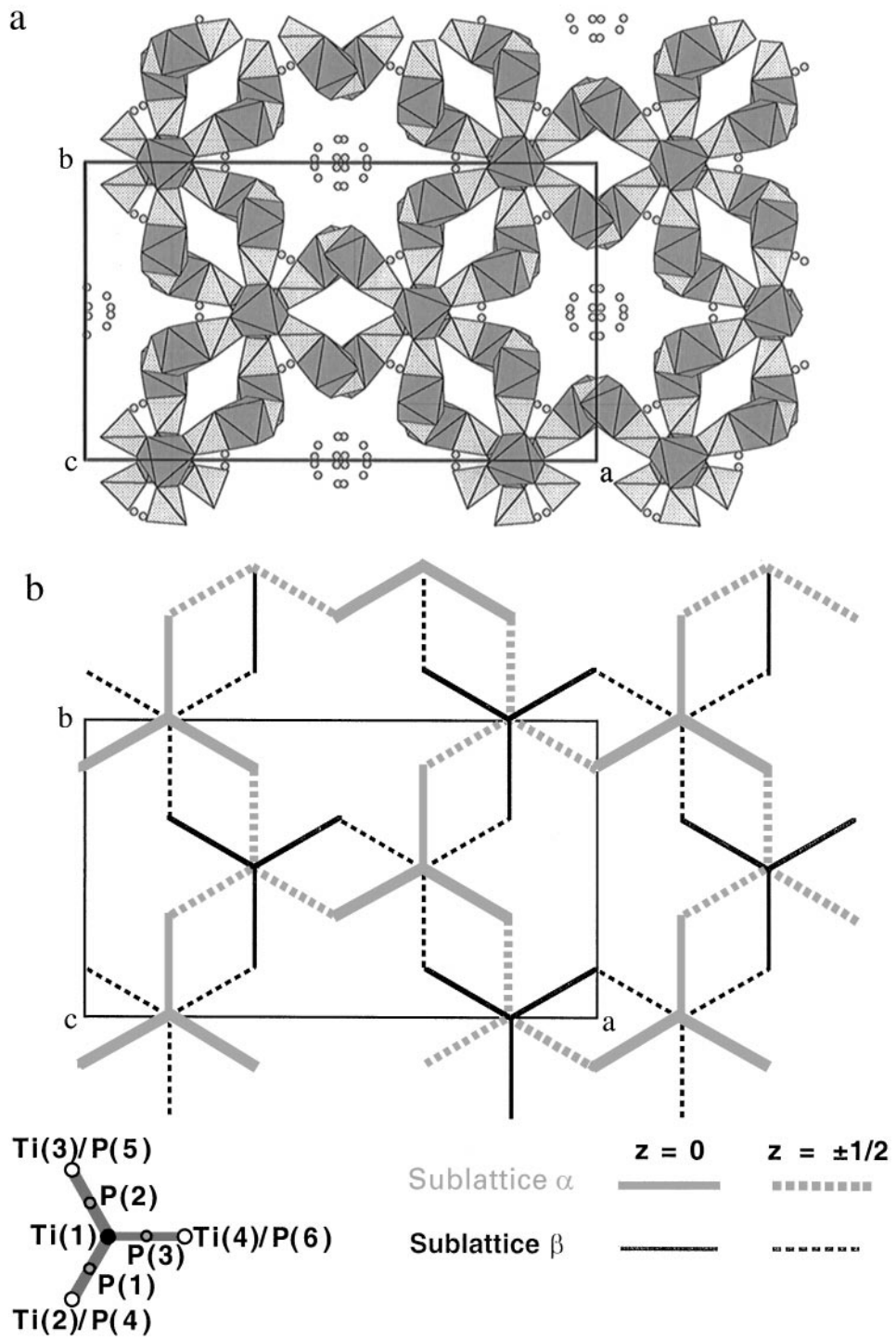

FIG. 1. (001) projections of the $AgTi_2(PS_4)_3$ structure: (a) interlocked chains of edge-sharing TiS_6 octahedra and PS_4 tetrahedra, small circles represent Ag atoms; (b) schematic view of the two interlocked sublattices.

bonds are much stronger, $\langle Ag\text{–}S\rangle = 2.53\text{Å} < r_{Ag^+} + r_{S^{2-}} \approx 2.80$ Å (21), so silver atoms are found in distorted sites along the wide tunnels, explaining the skeleton distortion.

$Ag_2NbTi_3P_6S_{25}$ structure exhibits only small-diameter tunnels hosting less than 2% of Ag atoms. The P_2S_6 entity, already reported in the titanium thiophosphate $Ti_4P_8S_{29}$ (27) and in the niobium thiophosphate NbP_2S_8-2D (28),

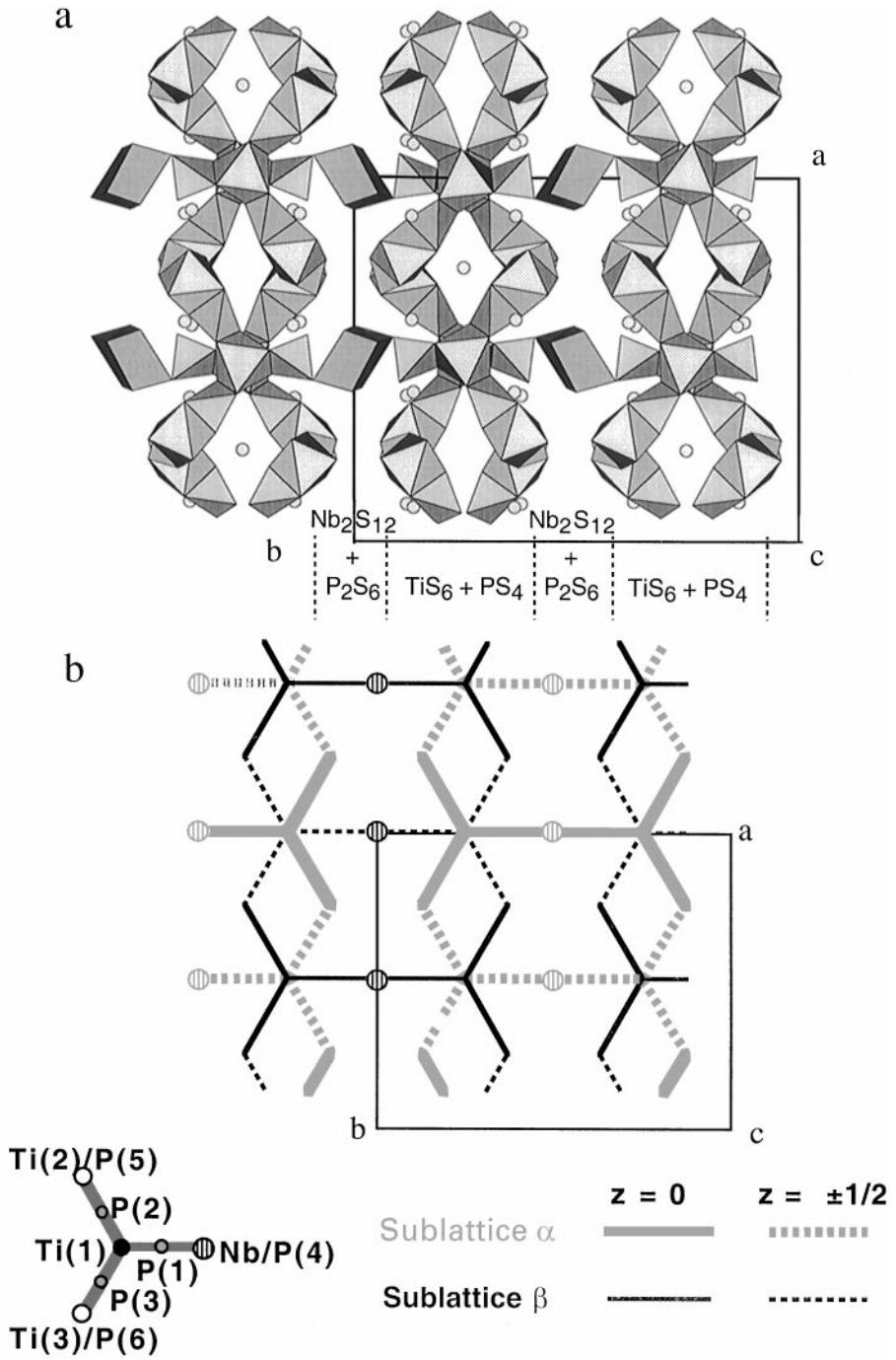

FIG. 2. (001) projections of the $Ag_2NbTi_3P_6S_{25}$ structure: (a) interlocked chains of TiS_6 octahedra, PS_4 tetrahedra, and Nb_2S_8 trigonal biprisms; (b) schematic view of the two interlocked sublattices.

presents here the shortest S–S distance (3.110 Å) between two unlinked sulfur atoms. The other polyhedral entity Nb_2S_{12} has been already reported in NbP_2S_8-2D (28), NbP_2S_8-3D (29), Nb_2PS_{10} (15), and $Nb_4P_2S_{21}$ (14). Its formation is due, on one hand, to the stabilization of the $4d^1$ electronic configuration of Nb^{IV} by a D_{3h} symmetry crystal field, as for V^{IV}–$3d^1$ in V_2PS_{10} (30), and, on the other hand, to the formation of $(S_2)^{2-}$ anionic pairs corresponding to the short bond S(1)–S(2) = 1.957 Å. In all reported Nb_2S_{12} entities, the Nb–Nb distance is very similar (2.859 to 2.884 Å), whatever the number of formed $(S_2)^{2-}$ pairs: two (28,29) or four (14,15,31). This distance is practically

TABLE 6
Extreme Values of Bond Lengths and Interbond Angles for the Anionic Polyhedra Both Present in the $AgTi_2(PS_4)_3$ and $Ag_2NbTi_3P_6S_{25}$ Structures

		$AgTi_2(PS_4)_3$	$Ag_2NbTi_3P_6S_{25}$
TiS_6 octahedra	bonds (Å)	$2.378 \leq Ti–S \leq 2.512$	$2.352 \leq Ti–S \leq 2.494$
	angles (°)	$81.1 \leq S\text{-}Ti–S \leq 110.3$	$80.3 \leq S–Ti–S \leq 111.2$
PS_4 tetrahedra	bonds (Å)	$1.980 \leq P–S \leq 2.116$	$1.973 \leq P–S \leq 2.075$
	angles (°)	$98.6 \leq S–P–S \leq 117.6$	$99.9 \leq S–P–S \leq 116.9$

unchanged in isotypic Nb_2X_{12} entities with different anions: 2.871 Å in NbS_2Cl_2 (32) and 2.89 Å in Nb_2Se_9 (33), like in the metal (2.863 Å) (34). Thus there is a real Nb^{IV}–Nb^{IV} bond with a d^1–d^1 magnetic coupling forming isolated cationic pairs in a diamagnetic solid. Stability of this Nb_2S_{12} entity may explain the failure of the synthesis of the "$AgNbTi(PS_4)_3$" phase with $AgTi_2(PS_4)_3$ structure type. These results justify the following writing of the oxidation states and charge balance: $Ag^I_4Nb^{IV}_2Ti^{IV}_6(P_2S_6)^{2-}(PS_4)^{3-}_{10}(S_2)^{2-}_2$.

It is noteworthy that we find in both structures the same TiP_3S_{12} unit built up from one octahedron sharing three opposite edges with PS_4 tetrahedra. This unit is the node of the interconnected polyhedra chains, inducing a particular space arrangement leading to the formation of interlocked structures. This phenomenon is reported in CrP_3S_{9+x} (35), built up from three interlaced sublattices made up with CrP_3S_{12} entities similar to TiP_3S_{12}; these three sublattices are linked to each other by van der Waals interactions only. In the present situation, one can see only two 3D-interlocked sublattices linked to each other by silver atoms forming ionocovalent Ag–S bonds. The two frameworks are $c/2$ shifted (about 5.8 Å). Figure 1b depicts the imbrication of the two sublattices, each of them built up from TiS_6 and PS_4 polyhedra sharing edges for $AgTi_2(PS_4)_3$. For $Ag_2NbTi_3P_6S_{25}$, imbrication is similar but only in (010) layers: the 2D sublattices are laterally linked to each other along b via Nb_2S_{12} entities (Fig. 2b).

In $ATi_2(PS_4)_3$ (A = Ag, Na), A^+ ions are located in the wide tunnels and are strongly delocalizable, inducing a high monodimensional ionic conductivity. Besides, the intertunnel migration pathways exhibit narrow "bottlenecks", inducing a low value of the tridimensional conductivity. The silver compound presents the best performance at high temperature, in accordance with the important quadrupolar distortion of Ag^+ ion (36) and its polarizability, 6 times higher than the Na^+ one (37,38).

CONCLUSION

The TiP_3S_{12} structural units (1 TiS_6 octahedron +3 PS_4 tetrahedra) exist in $AgTi_2(PS_4)_3$ and $Ag_2NbTi_3P_6S_{25}$ crystal structures, built up from anionic polyhedra sharing edges only. These TiP_3S_{12} units are the nodes of the two interlocked and independent sublattices; cohesion between them

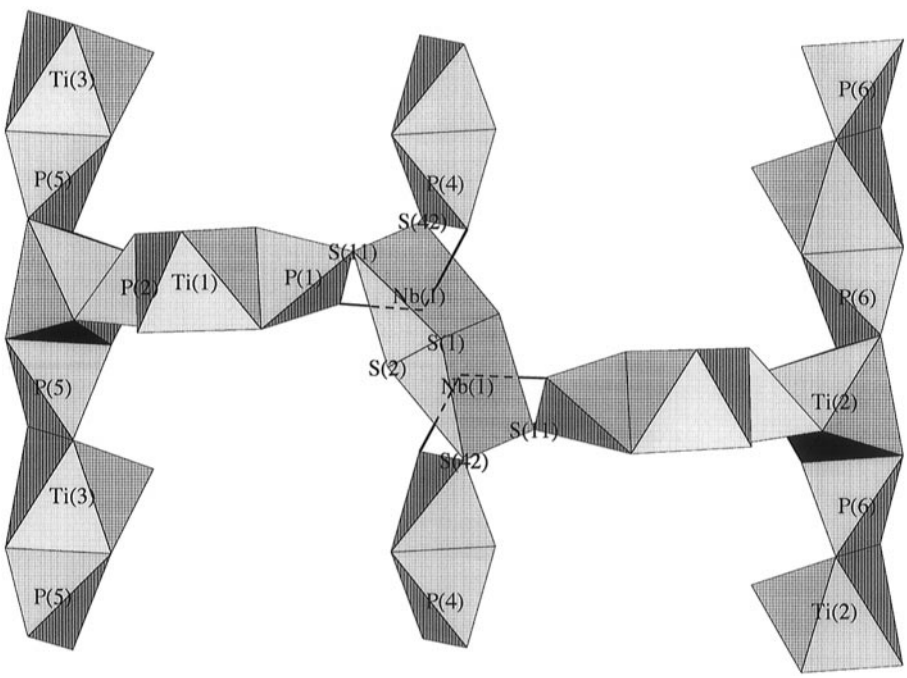

FIG. 3. Connection of two polyhedra chains by a tetracapped trigonal biprism Nb_2S_{12} also bonded to P_2S_6 bitetrahedron.

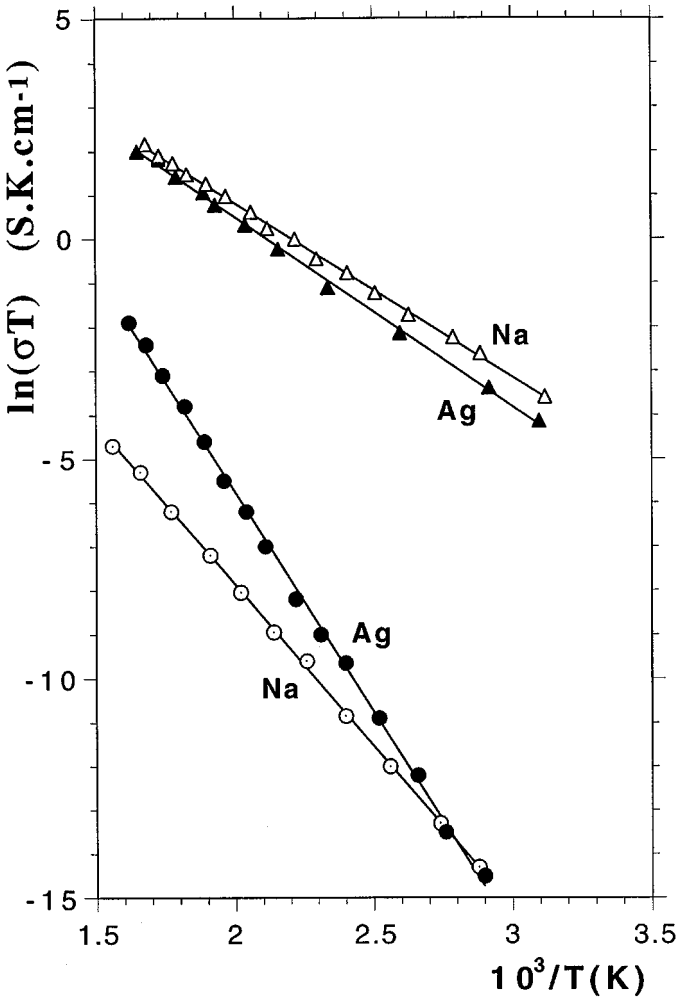

FIG. 4. Ionic conductivity vs temperature for $A\mathrm{Ti_2(PS_4)_3}$ compounds (A = Ag, Na) in the form of ceramics (circles) and single crystals along [001] (triangles).

is assumed to occur by S–Ag–S bridging bonds. The Nb^{IV} presence in $Ag_2NbTi_3P_6S_{25}$ leads to the formation of tetracapped trigonal biprisms Nb_2S_{12}, including two disulfide anions $(S_2)^{2-}$. This latter original structure is more compact than $AgTi_2(PS_4)_3$, characterized by a sulfur specific volume $V_{spe}(S) = 36.28$ Å^3 for $Ag_2NbTi_3P_6S_{25}$ and $V_{spe}(S) = 41.87$ Å^3 for $AgTi_2(PS_4)_3$.

The open $AgTi_2(PS_4)_3$ structure, isotypic with $NaTi_2(PS_4)_3$, exhibits very wide tunnels along [001] containing 46% of Ag^+ cations. These ions, weakly linked, can move easily and result in a high ionic conductivity along the c axis. Tridimensional conductivity is 1/200 as great as that along [001] due to the narrowness of interconnections between the wide tunnels.

Due to the great stability of the $[Ti_2(PS_4)_3]$ structural skeleton, insertion of various species may be considered. $LiTi_2(PS_4)_3$, $KTi_2(PS_4)_3$, $Ba_{0.5}Ti_2(PS_4)_3$, and $Ga_{0.33}Ti_2(PS_4)_3$ have been synthesized (39) and seem to be

TABLE 7

Ionic Conductivity (at 50°C and 300°C) and Activation Energy Values for Single Crystals and Ceramics of $AgTi_2(PS_4)_3$ and $NaTi_2(PS_4)_3$

	Single crystals; along [001]			Ceramics		
	$\sigma_{50°C}$ (S.cm^{-1})	$\sigma_{300°C}$ (S.cm^{-1})	E_a (eV)	$\sigma_{50°C}$ (S.cm^{-1})	$\sigma_{300°C}$ (S.cm^{-1})	E_a (eV)
$AgTi_2(PS_4)_3$	4.4×10^{-5}	0.9×10^{-2}	0.37	1.6×10^{-10}	6.8×10^{-5}	0.86
$NaTi_2(PS_4)_3$	8.5×10^{-5}	1.1×10^{-2}	0.34	3.5×10^{-10}	1.1×10^{-5}	0.63

isotypic with $NaTi_2(PS_4)_3$ according to their X-ray diffractograms. The presence of a reducible transition element in the skeleton allows insertion of an electropositive element. Our electrochemical intercalation results show that $A_{1+x}Ti_2(PS_4)_3$ (A = Li or Na for $0 \le x \le 2$) compositions can be reached (39). These new types of thiophosphates set up a wide structural family with high electrochemical potentiality.

ACKNOWLEDGMENTS

The authors thank particularly Dr. Sylvie Jaulmes for her assistance in crystal structure determinations and refinements.

REFERENCES

1. J. Rouxel, *in* "Intercalated Layered Materials" (F. Levy, Ed.), p. 201, D. Reidel, Dordrecht, 1979.
2. J. B. Goodenough, H. Y.-P. Hong, and J. A. Kafalas, *Mater. Res. Bull.* **11,** 203 (1976).
3. R. Brec, G. Ouvrard, A. Louisy, J. Rouxel, and A. Le Mehauté, *Solid State Ionics* **6,** 185 (1982).
4. M.-H. Whangbo, R. Brec, G. Ouvrard, and J. Rouxel, *Inorg. Chem.* **24,** 2459 (1985).
5. P. Colombet, A. Leblanc, M. Danot, and J. Rouxel, *J. Solid State Chem.* **41,** 174 (1982).
6. G. Burr, E. Durand, M. Evain, and R. Brec, *J. Solid State Chem.* **103,** 514 (1993).
7. P. Colombet, A. Leblanc, M. Danot, and J. Rouxel, *Nouv. J. Chim.* **7,** 333 (1983).
8. S. Lee, P. Colombet, G. Ouvrard, and R. Brec, *Mater. Res. Bull.* **21,** 917 (1986).
9. Z. Ouili, A. Leblanc, and P. Colombet, *J. Solid State Chem.* **66,** 86 (1987).
10. S. Lee, P. Colombet, G. Ouvrard, and R. Brec, *Inorg. Chem.* **27,** 1291 (1988).
11. E. Durand, M. Evain, and R. Brec, *J. Solid State Chem.* **102,** 146 (1993).
12. S. H. Elder, A. Van der Lee, R. Brec, and E. Canadell, *J. Solid State Chem.* **116,** 107(1995).
13. X. Cieren, J. Angenault, J.-C. Couturier, S. Jaulmes, M. Quarton, and F. Robert, *J. Solid State Chem.* **121,** 230 (1996).
14. R. Brec, M. Evain, P. Grenouilleau, and J. Rouxel, *Rev. Chim. Min.* **20,** 283 (1983).

15. R. Brec, P. Grenouilleau, M. Evain, and J. Rouxel, *Rev. Chim. Min.* **20,** 295 (1983).
16. J. de Meulenaer and H. Tompa, *Acta Crystallogr., Sect. A* **19,** 1014 (1965).
17. E. R. Howells, D. C. Phillips, and D. Rogers, *Acta Crystallogr.* **3,** 210 (1950).
18. G. M. Sheldrick, *SHELXS86*, *A program for the Solution of Crystal Structure*, University of Göttingen, 1986.
19. W. R. Busing, *Acta Crystallogr., Sect. A* **27,** 683 (1971).
20. P. J. Becker and P. Coppens, *Acta Crystallogr., Sect. A* **31,** 417 (1975).
21. R. D. Shannon, *Acta Crystallogr., Sect. A* **32,** 751 (1976).
22. E. Gaudin, L. Fischer, F. Boucher, M. Evain, and V. Petricek, *Acta Crystallogr., Sect. B* **53,** 67 (1997).
23. P. Toffoli, P. Khodadad, and N. Rodier, *Acta Crystallogr., Sect. B* **33,** 1492 (1977).
24. P. Toffoli, P. Khodadad, and N. Rodier, *Acta Crystallogr., Sect. B* **34,** 3561 (1978).
25. J. E. Bauerle, *J. Phys. Chem. Solids* **30,** 2657 (1969).
26. C. Wagner, "Proceedings, 7ème Comité International de Thermodynamique et de Cinétique Electrochimique," Lindau, Allemagne, 1955.
27. M. Z. Jandali, G. Eulenberger, and H. Hahn, *Z. Anorg. Allg. Chem.* **530,** 144 (1985).
28. P. Grenouilleau, R. Brec, M. Evain, and J. Rouxel, *Rev. Chim. Min.* **20,** 628 (1983).
29. M. Evain, R. Brec, G. Ouvrard, and J. Rouxel, *Mater. Res. Bull.* **19,** 41 (1983).
30. R. Brec, G. Ouvrard, M. Evain, P. Grenouilleau, and J. Rouxel, *J. Solid State Chem.* **47,** 174 (1983).
31. J. Do and H. Yun, *Inorg. Chem.* **35,** 3729 (1996).
32. J. Rijnsdorp, G. J. de Lange, and G. A. Wiegers, *J. Solid State Chem.* **30,** 365 (1979).
33. A. Meerschaut, R. Berger, and J. Rouxel, *Acta Crystallogr., Sect. B* **35,** 1747 (1979).
34. NBS Monogr. (*U.S.*) **25,** 1967 (1984).
35. P. Fragnaud, M. Evain, E. Prouzet, and R. Brec, *J. Solid State Chem.* **102,** 390 (1993).
36. P. W. M. Jacobs, *M.R.S. Bull.* **31,** 72 (1989).
37. J. R. Tessman and A. H. Kahn, *Phys. Rev.* **92,** 890 (1953).
38. J. Pirenne and E. Kartheuser, *Physica* **30,** 2005 (1964).
39. X. Cieren, Thèse de l'Université Pierre et Marie Curie, Paris, 1996.